PERGAMON

Journal of Structural Geology 22 (2000) 1297–1309

JOURNAL OF STRUCTURAL GEOLOGY

www.elsevier.nl/locate/jstrugeo

On the dynamics of magma mixing by reintrusion: implications for pluton assembly processes

George W. Bergantz

Department of Geological Sciences, Box 351310, University of Washington, Seattle, WA 98195, USA

Received 23 August 1999; accepted 15 March 2000

Abstract

Many plutons have formed by repeated intrusion, with complex internal contacts characterized by sharp and diffuse kinematic and compositional domains. We performed numerical experiments of mixing following magma chamber recharge that explicitly considers the fluid dynamics of multiphase mixtures. In the limit of zero diffusivity of intensive scalar quantities and low Stokes number, mingling by fluid instability is equivalent to deformation, and persistent fluid structures are kinematic 'attractors'. Three distinct regimes are exemplified, and can be described by their multiphase Reynolds (or Grashof) number. For a Reynolds number greater than about 100, an internal intrusive contact will collapse by internal wave-breaking, and chaotic magma mingling and mixing yield a nearly chamber-wide stratification. This flow may scour mushy regions at the walls and widely distribute previously crystallized material. For Reynolds numbers from 10 to 100, the internal wave does not break, and the stratification occupies less of the chamber, leaving islands of unmixed material. For Reynolds numbers around 1, internal slumping and folding can occur, and is the most likely to be preserved by a mineral fabric. Internal, sub-vertical contacts require a high absolute viscosity in the resident magma, representing a time-break between episodes of reintrusion. The shape of perched mafic domains captures the progress of sinking from higher levels into regions of increasing strength and crystallinity.

1. Introduction

One of the primary objectives of the structural analysis of plutonic rocks is to determine the dynamics and relative timing of magma ascent and emplacement. Regardless of the mechanism of magma ascent, many granitoid plutonic bodies result from a process of progressive assembly by the accumulation of magma. Evidence to support this notion comes from both structural and geochemical studies of plutons (Harry and Richey, 1963; Mahmood, 1985; Hill, 1988; Ramsay, 1989; Shimizu and Gastil, 1990; Bergantz, 1991; John and Stunitz, 1997; Macias, 1996; Paterson and Miller, 1998; Yoshinobu et al., 1998). In regions of putative melt generation and transport, sheet-like granite bodies have been reported (D'Lemos et al., 1992; Brown and Solar, 1998; Sawyer, 1998), and these can be heterogeneous mixtures of mafic and felsic domains (including restite) with a near-vertical aspect. These observations motivate us to consider a number of questions: What controls the dynamic mixing and mingling between magma batches during melt generation, transport and final emplacement? Can magma parcels retain their identity during emplacement in a rheologically heterogeneous framework? How much mixing will occur during reintrusion and interface collapse in regions of repeated and long-lived magma input? What stages of this process are recorded by a mineral fabric?

The identification of distinct kinematic and compositional domains are central to addressing these questions. Both horizontal and near-vertical internal contacts are commonly reported, and these are expressed as both sharp and gradational internal contacts (Bergantz, 1991). Contacts between structural-compositional domains are of special interest as they

E-mail address: bergantz@u.washington.edu (G.W. Bergantz).

0191-8141/00/$ - see front matter
PII: S0191-8141(00)00053-5

are an explicit manifestation of the rheological and dynamic contrasts and conditions just prior to solidification. The interpretation of internal contacts is complicated by the fact that plutonic rocks can carry information from processes that might operate simultaneously: within magma chamber processes such as convection, compaction and hyper-solidus flow (Sonnenthal and McBirney, 1998), syntectonic emplacement (Saint Blanquat (de) and Tikoff, 1997) and open-system processes such as reintrusion. In addition, Paterson et al. (1998) detail the difficulty of interpreting magmatic fabrics, especially in regard to the timing of the kinematic 'memory' and caution against over-interpreting kinematic elements in plutonic rocks to elucidate dynamic processes of ascent and emplacement.

Two approaches are used for analysis and interpretation of the magmatic assembly process: kinematic analysis of rock fabric, broadly defined, and dynamic analysis by forward modeling. The feed-back between the distribution of solids and the structure of a developing flow-field can be difficult to predict. This is the result of the two-way coupling where all the phases mutually interact and influence the flow field (Crowe, 1991; Vigneresse et al., 1996; Barboza and Bergantz, 1998). This has motivated the study of fluid–particle interactions in simple systems to elucidate the dynamical history of magma bodies. A number of experimental and numerical studies of multiphase flow at low Reynolds number (creeping flow) illustrate differing approaches and complexity (Freeman, 1985; Fernandez, 1987; Blumenfeld and Bouchez, 1988; Ildefonse and Fernandez, 1988; Ildefonse et al., 1992; Nicolas, 1992; Jezek et al., 1996; Arbaret et al., 1997; Fernandez and Fernandez-Catuxo, 1997; Ildefonse et al., 1997). The absence of a generality emerging from these studies highlights the difficulty of using shape-preferred orientations to uniquely describe even geometrically simple flows (Ottino, 1989).

The aim of the following sections is to elaborate on the conditions, controls and geological implications of multiple intrusion by magmas of similar composition, but differing density due to variations in crystal content. Of special interest are the dynamics and preservation of internal contacts in plutons. We develop some scaling relationships and evaluate their utility with a number of numerical experiments. The emphasis is on high-melt-fraction systems, which are likely to be the most dynamic. A secondary goal is to demonstrate the utility of numerical experiments of multiphase flow as a means of flow visualization in support of structural analyses. It should be appreciated that there is no 'best' description of mixing flows. They are usually considered in terms of either discrete vortices that stretch material lines by a rolling-up action, or a hierarchical structure or cascade of scales of motion, or even as structures such as filaments or highly stretched sheets. We will focus primarily on the vortex-based description, as it is likely to be of the most use in the interpretation of natural examples.

2. Previous work

Mixing can refer to the state of complete (molecular) homogenization, but our use is not that restrictive. We use the term mixing in the macroscopic sense to describe any volume where mass associated with premixing volumes is shared. The formulation we develop below is not capable of resolving mixing below the scale that is a multiple of the largest grain. For example, if a magma has crystals with a diameter on the order of a millimeter, the smallest averaging volume allowed by our approach would be on the order of a centimeter. This limit is consistent with the objectives given above, as we are primarily interested in the temporal development of the largest scales of flow; they are the most important in describing the distribution of phases and their orientation (Brown and Roshko, 1974).

Mixing is used to describe the processes of the folding and stretching of material surfaces, or their two-dimensional traces as lines. This is a consequence of the thinning of material volumes and their dispersal as a result of both shear and a process of sifting, which is the mutual interpenetration of volumes of differing mixture-density in a gravity field. This results in a creation of surface area and reduction of length scales that facilitates the smallest scales of mixing by molecular diffusion (Ottino et al., 1979). The physical volumes that undergo mixing are defined by their interfaces, and these can change shape and position with time. These interfaces are usually considered to be passive or active (Aref and Tryggvason, 1984). A passive interface is a surface of markers carried on the flow field without affecting the flow field itself. An active interface is one that delimits volumes of differing physical properties, and the presence of the deforming interface creates a feedback into the flow. Active interfaces can bound regions of distinct kinematic character. The metric of mixing is the local variation in the phase-volume-fraction. The local phase-volume-fraction is evaluated for a node whose minimum size is limited by formal averaging rules (Celmins, 1988).

In this work I will focus on conditions of maximum Reynolds number of $O(10^3)$. As discussed below, this is 'sub-turbulent' flow, as the Reynolds number is below the mixing transition of $O(10^4)$. The mixing transition refers to the development of pervasive small scale three-dimensional motion, and the value of the Lyapunov exponent, which is a measure of the exponential rate of increase in the surface area of an active interface, is always positive. For a Reynolds number

greater than the mixing transition, there are numerous theories that relate the strain rate of the smallest eddy to the value of the Lyapunov exponent. This stirring produces what is known as 'Eulerian chaos'. However, we will focus on flow at Reynolds number of O(1)–O(10^3) as this is relevant for a variety of geological applications and also a parameter range where a general model of the styles and efficiency of mixing has been elusive. Stirring that produces chaotic fluid pathlines at low Reynolds number is called 'Langrangian chaos'. Our goal is not to provide a comprehensive framework relating Reynolds number to Lyapunov exponent for moderate Reynolds number flow, but rather to offer qualitative insights into likely fluid structures that bear on the interpretation of plutonic contacts and geochemical zoning. Of additional interest are the phase velocity-scales of the motion and controls on the time-dependence of the flow.

Mixing in enclosures has been extensively studied, however few of these have considered the decay of potential energy as an explicitly multiphase process. Relevant works on mixing in enclosures as a result of initial conditions or boundary forcing include those of Danckwerts (1952), Bigg and Middleman (1974), McEwan (1983a,b), Ottino (1989), Duval (1992), Snider and Andrews (1994) and Linden et al. (1994). These works are of particular interest to structural geologists as they pertain to the kinematic description of a time-varying flow field. In the context of magma chambers, some models for magma mixing emphasized kinematic limits on complete homogenization (Sparks and Marshall, 1986; Frost and Mahood, 1987). Analog experiments have been a popular vehicle for visualizing the processes of reintrusion by fountaining from a narrow vent. The intrusion of magma chambers by magma fountains with differing viscosity contrasts has been considered by Campbell and Turner (1986). Huppert et al. (1986) modeled a variety of styles of injection and subsequent mixing in chambers with differing aspect ratios and conditions of stratification. These experiments are especially instructive as to the styles of stratification and entrainment that can occur during both laminar and turbulent magma injection.

In a study that deserves more recognition, the numerical experiments of Oldenburg et al. (1989) provide the first comprehensive assessment of time-dependent mixing of magmas that result from changes in chemical potential rather than the forced stirring by fountaining. A variety of statistical measures of mixing were introduced for application to magma mixing. Oldenburg et al. (1989) invoked the Boussinesq approximation, and this yields a system where the rate of production of mechanical potential energy (buoyancy) is explicitly coupled to the diffusion of scalar potentials, and a dynamic steady-state can eventually be realized with a loss of memory of initial conditions. However, this study did not consider the magma as an explicitly multiphase mixture, and our work complements and extends the simulations of Oldenburg et al. (1989) by explicit consideration of multiphase processes. In the models considered below, the potential energy for mixing results from the decay of an initial condition where the intrinsic density difference is dominated by variations in solid fraction. The physical boundaries are not scalar potentials of heat or mass, but are sources of vorticity. So the final state of the simulations considered here is the complete decay of mechanical potential energy. In other words, the mixture Reynolds number starts out at zero, reaches some maximum, and then decays to zero during one cycle of (re)intrusion.

3. Scaling relations

Fig. 1 shows the geometry of the system of interest. A resident magma with 30 vol.% crystals has been intruded by another crystal-free magma of similar bulk composition. This creates an unstable interface of height H. The scales of the initial, inertially dominated motion between the two bodies can be determined by equating the change in potential energy to kinetic energy, or more simply, by the difference in hydro-

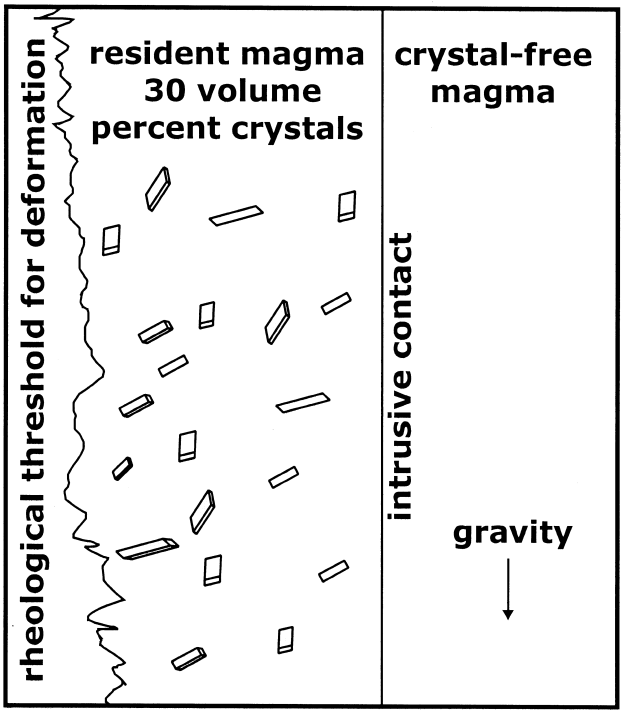

Fig. 1. A diagram of the model of the intrusive system is shown. A region of constant crystallinity is bounded on the left by the wall of the crystallization front with roughness exaggerated, and on the right by a strip of reintruded, crystal-free material. This is the starting condition of Figs. 2–5.

static pressure gradients to the initial velocity scale,

$$\Delta P = (\rho_r - \rho_i)gH,\ \Delta P \approx \bar{\rho}u^2. \tag{1}$$

This yields the usual hydraulic scaling for the local average velocity u

$$u = \sqrt{gHA_t}, \tag{2}$$

where g is the scalar acceleration of gravity and the Atwood ratio for a multiphase mixture is defined by

$$A_t = \frac{\rho_r - \rho_i}{\rho_r + \rho_i},\ \rho_r = \varepsilon_{lr}\rho_{lr} + \varepsilon_{sr}\rho_{sr},\ \rho_i = \varepsilon_{li}\rho_{li} + \varepsilon_{si}\rho_{si}. \tag{3}$$

The subscript ε is volume fraction, r and i are for mixture quantities of resident and intrusive magma, respectively, and l and s are liquid and solid and starred variables refer to phase, not mixture, properties. The time scale for this initial motion is

$$t_i \approx \sqrt{\frac{H}{gA_t}}, \tag{4}$$

and the system Reynolds number is

$$\mathrm{Re}_H \approx \frac{Hu}{\bar{\eta}} = \frac{H}{\bar{\eta}}\sqrt{gHA_t} = Gr^{1/2}, \tag{5}$$

where Gr is the Grashof number and the system kinematic viscosity is defined as

$$\bar{\eta} = \frac{\mu_r + \mu_i}{\rho_r + \rho_i},\ \mu_r = \varepsilon_{lr}\mu^*_{lr} + \varepsilon_{sr}\mu^*_{sr},\ \mu_i = \varepsilon_{li}\mu^*_{li} + \varepsilon_{si}\mu^*_{si}. \tag{6}$$

The Reynolds number used here is different from the one used in Huppert et al. (1986) as that Reynolds number depends on the volume rate of reintrusion of new material. The scale relations given above will hold until the flow is penetrated by the viscous effects from the presence of the boundary. This will take place at a time of order

$$t_v \approx \frac{H^2}{\bar{\eta}}. \tag{7}$$

Dimensionless velocity and time can be obtained by normalization with Eqs. (2) and (4), respectively.

Variations in the Reynolds number, or Grashof number, reflect changes in the physical geological system. For example, if the melt phase has a density of 2440 kg/m^3, the solid phase a density of 2700 kg/m^3 a contrast in crystallinity of 30 vol.% yields an Atwood ratio of 0.0157. For many applications of interest in magmas, the Atwood ratio will be around 0.02. For a liquid dynamic viscosity of 10^4 Pa s and an internal contact height of 126 m, the Reynolds number would be 100. If the viscosity is an order of magnitude higher at the same vertical length scale, the Reynolds number would be an order of magnitude lower.

In this study, heat transfer will be neglected. Temperature can control the time-rate of decay of potential energy by changing the density of the melt phase and by influencing the magma viscosity by changes in melt composition and numbers of phenocrysts through resorbtion and crystal growth. However, these are minor as changes in melt composition and solid volume fraction will have much more influence than temperature (explicitly) on viscosity and density. If fluid motion is sufficiently rapid, the within-phase change of extensive quantities between the mixing volumes can be ignored. It is important to note that for a system in equilibrium, the spatial distribution of the solids can be arbitrary (Hills and Roberts, 1988) and so variations in local volume fraction that result from flow do not require any change in chemical potential. The buoyancy associated with temperature changes is much less than that associated with variations in crystallinity. For the examples considered below, the mechanical potential energy associated with the variations in crystallinity is an order of magnitude greater than that associated with likely temperature differences. In summary, the thermal field is carried on the flow, as thermal diffusion is much less rapid than the rate of advective transport. This is equivalent to the high Peclet number assumption.

4. Numerical experiments

Numerical simulations are offered in support of the scaling results given above and to illustrate the temporal character of the flow field. The governing equations and model assumptions are discussed in the Appendix A. The model is an extension of the Eulerian–Eulerian two-phase model of Ni and Beckermann (1991), which is a variation of the theories of Ishii (1975), Hassanizadeh and Gray (1979) and Drew (1983). This two-phase theory assumes that all space can be occupied by both phases, and that the local phase volume fraction is a continuous variable that represents the existence probability of the phase in any spatial volume that defines a stationary average. Within this volume each phase has a distinct velocity, but that velocity is single-valued for all local material elements of that phase.

Five sets of simulations are given below, each illustrating a distinct dynamic regime following reintrusion. All the simulations have the same initial configuration as shown in Fig. 1: A more dense, crystal-rich region of resident magma on the left, and a less-dense, crystal-poor, just-intruded magma on the right. This initial condition is somewhat arbitrary, but as near-vertical contacts are observed in nature, and chambers must be

intruded by less dense material that will rise up against a magma chamber roof, e.g. Hogan et al. (1998), this initial condition is a reasonable one. The analog experiments of Huppert et al. (1986) suggest that some entrainment must have accompanied reintrusion to produce this initial condition. We agree, but propose to evaluate a simple case, as any assumptions are equally arbitrary. Changing the initial density contrasts to reflect some prior and unconstrained entrainment is a trivial addition. We have evaluated the influence of having both resident and reintruded material be crystal-bearing and it has virtually no impact on the generalizations offered below if one (re)defines the scale properties accordingly.

This configuration in Fig. 1 is dynamically unstable and the resident, denser, crystal-rich magma will slide under the less-dense, intruded magma. It is this exchange of position that leads to interface collapse and mixing of the two volumes. The boundary condition for the liquid phase is no-slip at the upper and left-hand boundaries. Slip is allowed on the lower boundary and the right wall. These regions of slip imply that the right-hand boundary is a reflecting boundary, and the bottom of the domain is perhaps a region of deformable crystal mush. The boundary condition for the tangential component of the solid phase velocity is zero on the upper and left-hand boundary. This is equivalent to assuming that the surface roughness scale is greater than the diameter of the crystal, effectively creating a trapping condition (Ding and Gidaspow, 1990).

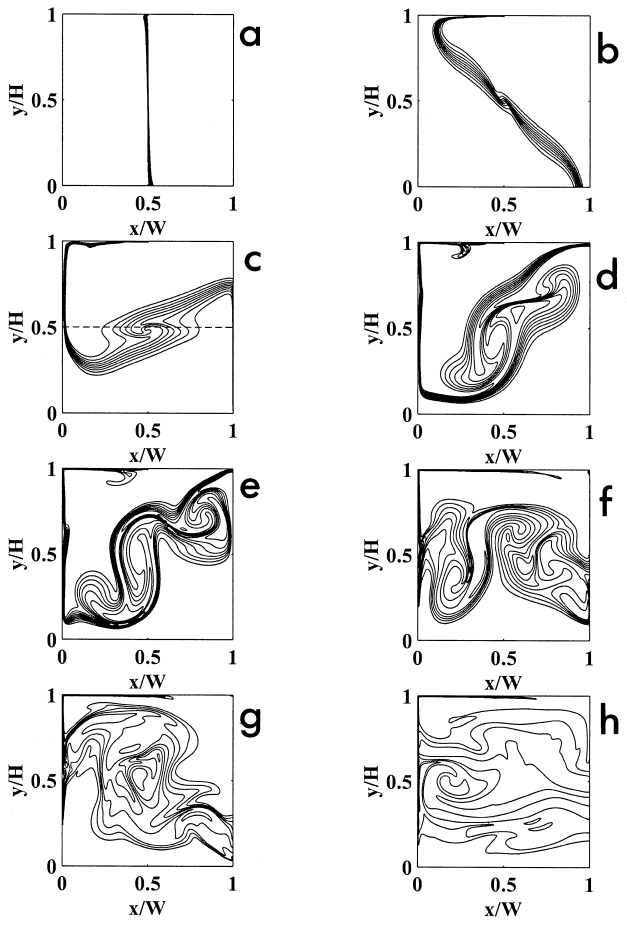

Fig. 2. The collapse of the intrusive contact for a Reynolds number of 1000. The contours are volume percent liquid, equally spaced from 0.7–1. See text for discussion. The dimensionless time, $t*$, is the actual time divided by the scale time in Eq. (4). (a) $t*=0.1$, (b) $t*=1.0$, (c) $t*=1.9$, (d) $t*=3.1$, (e) $t*=3.7$, (f) $t*=5.0$, (g) $t*=6.2$, (h) $t*=14.9$.

The first case we will consider is the most dynamic and illustrates many of the features associated with time-dependent, chaotic mixing. Fig. 2(a)–(h) illustrate the progressive folding and mixing that result from the collapse of the intrusive contact. The contours are constant liquid-volume-fraction. The system Reynolds number is 1000, and the flow is inertially dominated during the most dynamic period. Fig. 2(a) and (b) depict the start of interface collapse as the flow-field begins as a simple, counter-clockwise rotation. The initial intrusive contact is stretched and begins to thicken as a result of the inter-penetration of the resident and intruded magma volumes. The liquid-fraction contours are compressed at the top as a consequence of the no-slip upper boundary condition.

The transformation of potential energy to kinetic energy yields sufficient momentum to the resident magma that it over-shoots the line of neutral stability as illustrated in Fig. 2(c). This leads to the formation of an internal wave and the interface will continue to steepen, yielding a Kelvin–Helmholtz type of instability by virtue of mutual shear across the interface mixing zone. This process is just beginning in Fig. 2(c), and the vorticity associated with the formation of this wave is manifested as the elliptical roll-up of the contours in the center of the figure. This roll-up is very similar to what is called a 'whorl' (Khakar et al., 1986; Ottino, 1989) and dramatically increases the efficiency of mixing by enhanced rotational stretching (strain) of material lines. It is during this period that the maximum velocity occurs, and the observed maximum was about 80% of the velocity scale given in Eq. (2), indicating good agreement between scale results and more detailed model results.

In Fig. 2(d) the interface has been completely disrupted and thickened. Although the center of the internal-wave has the dominant vortex, opposing subsidiary pairs of vortices have been generated forming a composite structure of (at least) three vortices. The one in the lower-left rotates clockwise, the one in the upper-right, counter-clockwise. These are similar to 'blinking vortices' (Aref and Tryggvason, 1984). It is the formation and unsteady motion of these vortices that enhance mixing throughout the chamber, and pro-

duce temporal and spatial chaotic mixing. The highly stretched and folded portions are called 'tendrils' and taken together, this kind of flow is known as 'whorl and tendril' flow. The length of the interface has become very stretched relative to its initial length, and the mixing region involves about a third of the cavity, although 'islands' persist wherein there has been no mixing.

In Fig. 2(e) the composite vortex structure is oscillating: It is swept to the left as the center of mass is still above the level of neutral buoyancy. This sloshing of the composite structure breaks it up into many smaller vortices as shown in Fig. 2(f). This type of chamber-wide quasi-periodic behavior is more efficient at mixing than steady flow, as the suite of vortices are swept about the chamber (Chien et al., 1986). In Fig. 2(g), a large central vortex emerges as the dominant structure. Eventually, the kinetic energy decays by work done against viscous drag and produces a nearly stable stratification as shown in Fig. 2(h). At this time, most of the cavity is occupied by a mixture of material from both the resident and re-intruded magma. No evidence of the initial vertical intrusive contact remains, except for a highly sheared and thin region at the left-hand and upper boundaries.

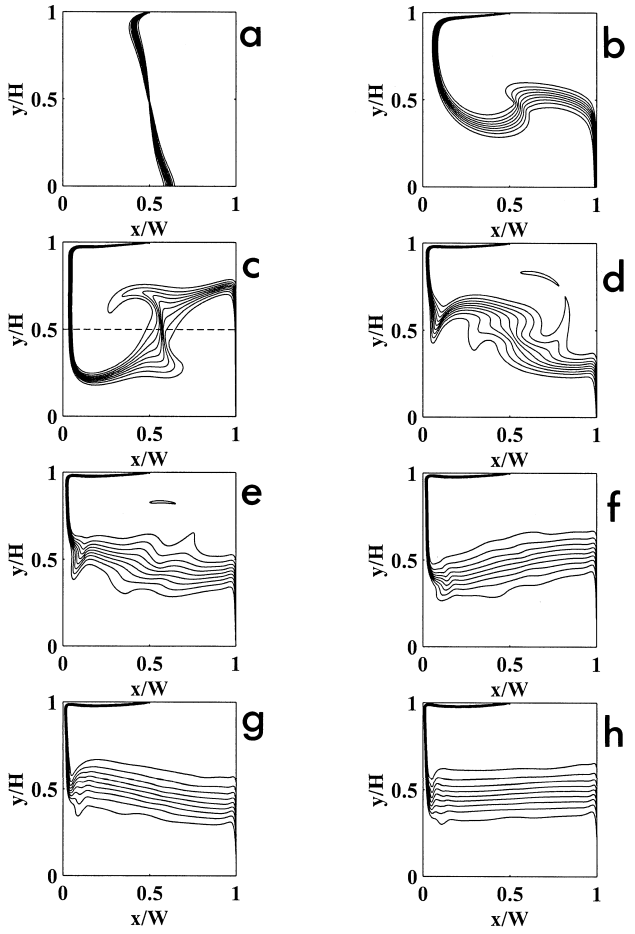

Fig. 3. The collapse of the intrusive contact for a Reynolds number of 100. Contour spacing same as Fig. 2. See text for discussion. The dimensionless time, $t*$, is the actual time divided by the scale time in Eq. (4). (a) $t*=0.8$, (b) $t*=3.1$, (c) $t*=3.9$, (d) $t*=7.8$, (e) $t*=11.8$, (f) $t*=15.7$, (g) $t*=19.6$, (h) $t*=31.4$.

The strain history and temporal morphology of the flow-field can be considered to be a combination of a Rayleigh–Taylor (R–T) instability with an over-turning motion. However, unlike the ideal R–T case, there is no preferred wavelength to excite the over-turning motion that dominates the mixing at early times in R–T simulations. As a result, there is not as much shearing and mutual interpenetration until the vortices have appeared that result from wave-breaking. Hence, the growth of the instability and the efficacy of mixing are different. Bergantz and Ni (1999) have considered the multiphase R–T case and a number of the features discussed here are present in those simulations. Despite there differences at early times, both simulations illustrate the development of non-topological elements, which leads to the formation of islands of variably mixed material. Once formed, they can persist in an otherwise complex flow (Ottino et al., 1988).

In the next case the Reynolds number was 100. Fig. 3(a)–(h) illustrates the temporal development of this regime. In Fig. 3(a)–(c) an internal wave is formed with a pronounced cusp, but unlike the previous case, the wave does not break as the bulk oscillation rotates the wave out from under the cusp. The cusp remains as a perched region that eventually is distributed by subsequent shear, and the interface remains topological. Prior to the complete penetration by boundary viscous effects, the interface region is like a damped oscillator, and the period of this oscillation for aspect ratio equal to one is:

$$t_0 \approx \frac{H^2}{\mathrm{Re_H}\bar{\eta}}. \tag{8}$$

The flow field becomes highly stretched during laminar oscillation. The flow is too weak to produce the whorl-and-tendril morphology, and shear stresses are not sufficient for Kelvin–Helmholtz instabilities to form that would cause thickening of the interface and the formation of multiple vortices. The final state of the system is horizontal stratification, but with much larger islands of unmixed material than in the higher Reynolds numbers case.

The complexity of the flow and mixing efficiency will change at higher Reynolds numbers. Turbulent mixing is characterized by the simultaneous presence of vorticies of differing sizes. However, as pointed out by Moses et al. (1993), despite Reynolds numbers of up to 10^4, local domains of buoyancy may still be essentially laminar and viscosity important. It is their mutual interaction throughout the chamber that gives

rise to the diverse structures typical of turbulence. This is a consequence of the large, outer scales of flow not being well separated from the inner, kinetic energy dissipation scales. At a Reynolds number above 10^4, the mixing transition is reached and the turbulence is fully developed. This complexity is difficult to characterize, and is usually described as global or superimposed (multi)fractal structures (Feder, 1988; Linden et al., 1994) or by specification of a Lyapunov exponent for a bounding contour of an advected scalar quantity.

There are a number of ways to define the efficiency of mixing. One would be to divide the thickness of the stratification after wave-breaking by the wave amplitude. For the first case, this yields an efficiency of about 0.7. In the second case, it was about 0.5. These values are higher than those previously reported for mixing in an enclosure, because no work is done against viscosity at the reflecting boundary conditions at the right side and bottom. If the right side and bottom were no-slip boundaries, these numbers would decrease by about half, giving values within the limits proposed by McEwan (1983a).

Numerical simulations were also preformed for Reynolds numbers of 1, 0.1 and 0.01. The solutions are not shown in the interest of brevity but will be briefly described. For a Reynolds number of 0.1 and 0.01, the exchange of position produced negligible mixing as there was little vorticity produced. The resident and intruded magmas simply slipped past each other under conditions of nearly creeping flow producing a fairly sharp interface between the two. There is negligible transfer of momentum or mass between the resident and intruding magma as a result of the decay of position potential energy. Because there is no increase in surface area, the sharing of scalar potentials, such as temperature or concentration, will be described by a length scale like that of the global size of the body.

The fourth case provides some insights into the structure of the flow in a chamber that is shaped like a sill. Fig. 4(a)–(d) have the same initial conditions as

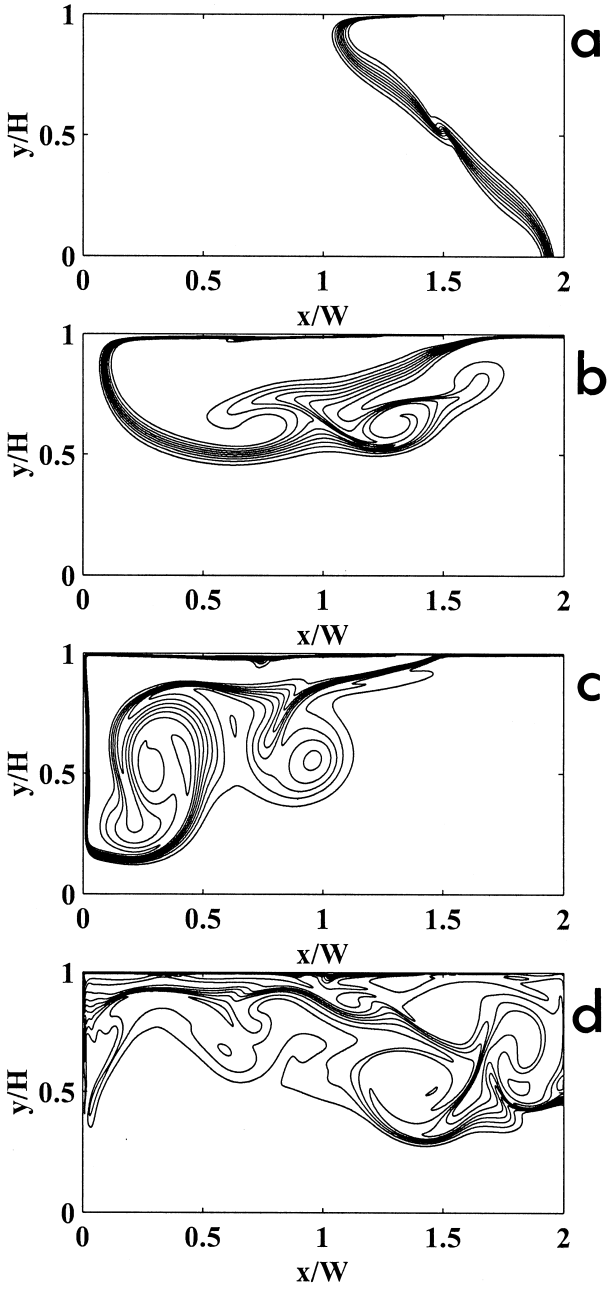

Fig. 4. The collapse of the intrusive contact for a Reynolds number of 1000 and an aspect ratio of 0.5. Contour spacing same as Fig. 2. See text for discussion. The dimensionless time, $t*$, is the actual time divided by the scale time in Eq. (4). (a) $t*=1.0$, (b) $t*=3.1$, (c) $t*=5.0$, (d) $t*=10.4$.

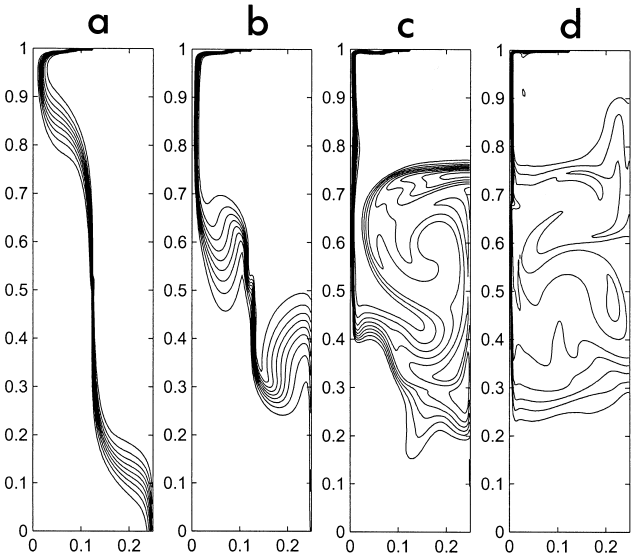

Fig. 5. The collapse of the intrusive contact for a Reynolds number of 1000 and an aspect ratio of 4.0. Contour spacing same as Fig. 2. See text for discussion. The dimensionless time, $t*$, is the actual time divided by the scale time in Eq. (4). (a) $t*=0.6$, (b) $t*=1.0$, (c) $t*=2.5$, (d) $t*=7.4$.

the first case: the height-based Re is equal to 1000. However the width is twice that in the first case, so the aspect ratio is 0.5. This change in width changes the chamber-wide, integrated potential energy, and so this simulation is not directly comparable to the previous examples. However, it still provides a useful and geologically important example of reintrusion that warrants consideration. As we would expect, at early times the flow is nearly identical with the first case, compare Fig. 2(b) with Fig. 4(a). In Fig. 4(b), the less dense material moves along the upper boundary, trailing a pair of vortices. If there were no vertical wall to eventually impede the flow, it would simply 'run out' like a slump. In Fig. 4(c), the reintruded material has arrived at the left wall, and the momentum has curled the flow up into a large central vortex; the trailing vortices in Fig. 4(b) are just arriving. The flow will continue to oscillate and Fig. 4(d) illustrates the return of the wave to the right hand side. This will continue until a stable stratification is achieved. The region that is occupied by the stratification is less than in the first case, but the results are qualitatively similar.

The fifth simulation, shown in Fig. 5, is for flow in a vertical slot of aspect ratio 4. This might be appropriate for conditions in a vertical magma feeder. The simulation is the same as in the first case, Re equal to 1000. The dominant structure is a single whorl that is centered nearly at the right hand margin, as the no-slip left-hand boundary does not allow for subsidiary structures to form. This process ultimately decays yielding a stratified region that occupies the center of the conduit. Note the minor R–T instability that is dripping from the upper-right corner, like that seen in Fig. 2(e). These second-order instabilities will continue to stir and perturb the mixture, once the main motion associated with reintrusion is nearly exhausted (Bergantz and Ni, 1999).

5. Implications for geological systems

The simulations offered here exemplify some of the dynamics that can occur during reintrusion, and illustrate the difficulties structural geologists face in uniquely interpreting kinematic data from plutons. Among the most important points is that the preservation of sharp, near-vertical internal contacts requires not just a large rheological contrast, but a high absolute viscosity for the resident magma. This requires that the resident magma be virtually solid or have a sufficiently low melt fraction that grain–grain contiguity is achieved and provides a supporting framework. This requirement allows one to estimate a time scale for mixing following reintrusion: It must be on the order of the cooling time for the body of resident magma. Applying the conduction cooling relationship provides a conservative estimate for this time for a body with length scale L:

$$t \approx \frac{L^2}{\kappa}, \tag{9}$$

where κ is the thermal diffusivity modified to include the latent heat of crystallization. This implicitly assumes that the magma has a linear melt-fraction to temperature relationship, although that is not a particularly restrictive condition (Bergantz, 1990). Reintrusion on time scales less than this may lead to partial or complete interface collapse and would not yield distinctive internal contacts. A corollary of this is that one need not expect any simple geochemical genetic relationship between elements in a vertically sheeted, multiply intruded suite. Both sharp and transitional horizontal contacts have been reported in ash-flows and can result from reintrusion, without calling upon a box-filling mechanism like side-wall crystallization (Eichelberger and Wiebe, 1999). Stratification is an inevitable consequence of reintrusion by more evolved or volatile-rich magmas. Hence, any shared, near-liquidus geochemical characteristics may have originated in a region of common melt generation, rather than result from an in-situ process. And the presence of diverse magma types with complex internal contacts suggests that the dominant shared characteristic of the system is a persistent geographical locus of magmatism rather than a parent magma.

Prior to reintrusion, if the margin of the body has a transitional character from completely solidified to liquid-crystal mush, it is possible that interface collapse could erode, or scour, this contact back to a region where the solid fraction is high enough to be effectively rigid. This scouring would disaggregate 'mushy' portions of the margin and mix it with the intruding magma. This is a mechanical process like the 'defrosting' proposed by Mahood (1990) in that it provides a means for juxtaposing phenocrysts with differing parent magmas, growth ages and zoning profiles. In this case, a sharp internal contact represents a surface of high strength, exhumed by shear stresses associated with the 'viscous wind' of circulation. For this case the length scale in Eq. (9) would be that portion of the body that lies between the internal surface of high strength and the magma to country-rock contact.

One of the non-intuitive implications of these simulations is that the case of weak flow may provide for the most complex and lasting expression of this process in the kinematic character of the pluton. Flow at Reynolds number of order 1 or less will be creeping flow, characterized by a slow folding, and likely occurs in regions where the solid fraction has nearly reached contiguity. This type of flow is more likely to reveal spatially and tem-

porally variable increases in strength, and exhibit ductile behavior. This could produce internal folds and slumps that would be preserved, unlike the more dynamic cases where the entire flow field is reset until the potential energy decays. Following Paterson et al. (1998) it seems likely that only the low Reynolds configuration will be preserved in the plutonic stage. Thus, the gradational contacts that are present in some concentrically zoned plutons (Shimizu and Gastil, 1990), may represent this process. These results re-emphasize the fact that subvertical internal contacts represent processes that occur at the close of a magma chamber cycle, or during a rejuvenation of activity.

Although the simulations were for reintrusion by less dense materials of like composition, the results are general and can be (cautiously) extended to some aspects of mafic–felsic interaction. Isolated and perched, higher density materials, like mafic enclaves, must represent the last stages of activity or mafic bits that have been captured by a crystallization front. Larger mafic domains, like the 'North America' on the face of El Capitan, Yosemite National Park, California, are sitting in a region of higher strength and crystallinity, and perhaps are frozen in the act of tunneling downward, or obliquely, through regions of variable strength and melt fraction as 'magma worms' (S.R. Paterson, personal communication). Many mafic domains may represent regions that are arrested while falling through their host, providing an efficient way to mingle and mix magmas (Wiebe and Ulrich, 1997). It is also evident that the floor-layers and pipe structures mapped by Elwell et al. (1960), Vaughan et al. (1995), Bremond d'Ars and Davy (1991) and Wiebe and Collins (1998) must have solidified before any tilting of the magma chamber took place. If tilting had occurred prior to solidification, the mafic material would droop in place, and collapse the delicate pipes of silicic material. Thus, the tilting is probably uncoupled from the magma chamber forming process, or happening so slowly that the bottom boundary of the magma chamber is cooling faster than the tilting. This places constraints on both the rate of tilting and on the rheology of the underlying country rock.

It is also evident that the intrusion of mafic material along the floor of a magma body is the least dynamic way to initiate volumetrically significant magma mingling for time scales a factor of 10–100 of Eq. (4). This is a consequence of the Reynolds approaching zero. Without large changes in the density contrast that accompany volatile exsolution, the only potential energy available for mixing is from temperature differences. The ratio of the position potential energy to that from temperature differences operating over the same vertical length is:

$$\frac{A_t}{\varepsilon_1 \beta \Delta T}, \tag{10}$$

where β is the thermal expansion coefficient for the melt phase and ΔT is a characteristic temperature difference. This ratio can have a value of order 10–100 illustrating the relative importance of position potential energy. However, thermal buoyancy will have different dissipative structures and time scales, and can be persistent if it is associated with a boundary condition rather than an initial condition. A more comprehensive assessment will be the subject of future communications.

How can one assess the geological verisimilitude of the models presented here? Unfortunately, dynamic systems often destroy the evidence of their origins. In addition, the absence of such stratification in the pluton does not mean that it did not exist at an earlier stage in the magma chamber. This will be especially true in magmatic systems at high melt fraction, before crystal contiguity sets-up a yield strength. With regard to the 'information theory' approach to magmatic systems (Petford et al., 1997), there may be no memory of this stage except for crystal zoning (Knesel et al., 1999), and even this may not yield a monotonic record of events due to crystal resorbtion. Nonetheless, crystal zoning studies, combined with structural studies of kinematic domains may prove useful in establishing the route(s) any magma parcel takes to final position in a pluton. Bands of stratified material occurred in all the simulations we considered and appear to be an inevitable consequence of reintrusion. However, stratification can also occur by side-wall fractionation (box filling), although the evidence of this has not been frequently documented in the plutonic record. Processes such as eruption or the falling of crystal rich plumes (Bergantz and Ni, 1999) from the roof could disrupt a stratification. So the absence of evidence is not a robust test. Probably the only way to test these notions would be in a system where reintrusion produces distinct isotopic domains (Hill et al., 1988; Hill and Silver, 1988), as reintrusion of magmas with similar major element compositions may be difficult to recognize in the field (Pembroke and D'Lemos, 1995)

Acknowledgements

I wish to acknowledge support from NSF grants EAR-9508291 and EAR-9805336. The University of Washington provided funding for my Beowulf cluster. Thanks go to J. Ni, R. Breidenthal, W. Duval and especially C. Crowe for discussions on numerical modeling and multiphase flow. S.R. Paterson, M. Brown, K.

Knesel, K. Fowler Jr., A.R. Robinson, W. Hirt and S. Barboza are thanked for discussions on plutonic rocks. The editorial assistance of J.C. White, and two anonymous reviewers is gratefully acknowledged. Special recognition to S. Macias for many memorable and enjoyable moments ruminating on these topics while standing on the outcrop in the Sierra Nevada.

Appendix A

The numerical simulations are based on the model conservation equations given below. The conservation of mass for a phase k can be expressed as

$$\frac{\partial}{\partial t}(\varepsilon_k \rho_k) + \nabla \cdot (\varepsilon_k \rho_k v_k) = 0, \tag{A1}$$

where t, ε, ρ, and v refer to the time, volume fraction, mass-averaged density, and volume-averaged intrinsic velocity vector, respectively.

The conservation of momentum for a phase k can be written as

$$\frac{\partial}{\partial t}(\varepsilon_k \rho_k v_k) + \nabla \cdot (\varepsilon_k \rho_k v_k v_k) = -\varepsilon_k \nabla P_k + M_k^d + \varepsilon_k \rho_k g + \nabla \cdot \left\{ \mu_k^* \left\{ \nabla(\varepsilon_k v_k) + \left[\nabla(\varepsilon_k v_k)\right]^t - v_s \nabla \varepsilon_k - \nabla \varepsilon_k v_s \right\} \right\}, \tag{A2}$$

where g refers to the acceleration due to gravity, and M_k^d refers to the dissipative part of the interfacial momentum transfer. We considered the resident magma to be a two-phase system of silicate liquid and solid silicate crystals where subscript k can be taken as l and s, respectively. We also assumed that there is instantaneous microscopic pressure equilibration which is appropriate if the speed of sound for each phase is large compared to the calculated velocities (Drew, 1983). The interfacial balance and momentum transfer may be modeled in terms of a drag coefficient

$$M_s^d = -M_l^d = -\frac{3}{4}\frac{\varepsilon_s}{d_s}\rho_l C_{d\varepsilon} |v_l - v_s|(v_l - v_s), \tag{A3}$$

where d_s is the diameter of the crystals, and C_{de} is the generalized drag coefficient which is valid for all solid fractions and includes the permeability after the solid crystals reach the contiguity limit and become stationary (Argwahl and O'Neill, 1988):

$$C_{d\varepsilon} = \left\{ \frac{24 \times 2C_{k\varepsilon}(1-\varepsilon_l)}{\mathrm{Re}} + C_{i\varepsilon} \right\}, \qquad \mathrm{Re} = \frac{\rho_l \varepsilon_l |v_l - v_s| d_s}{\mu_l}, \tag{A4}$$

where $C_{k\varepsilon} = 25/6$ and $C_{i\varepsilon} = 7/3$. We have ignored lift forces and changes in drag associated with synneusis and particle shape anisotropy (Schwindinger, 1999). These are not particularly difficult to implement, however little is known about their mutual influence when the carrier phase may be turbulent.

Based on the rheology of multiphase flow, both the liquid and mixture dynamic viscosity is assumed to be Newtonian at a given value of the solid volume fraction. There currently are not sufficient experimental data to generalize the strain-rate dependence of the viscosity for all crystal-bearing magmas. However, for a concentration of solids less than 30 vol.%, the assumption of Newtonian behavior may be appropriate; see discussion in Hallot et al. (1996). The liquid dynamic viscosity is taken as $\mu_l^* = \mu_l$ and the solid dynamic viscosity as

$$\mu_s^* = \frac{\left[1 - \varepsilon_s/\varepsilon_{sp}\right] - 2.5\varepsilon_{sp} - \varepsilon_l}{\varepsilon_s}\mu_l, \tag{A5}$$

where $\varepsilon_{sp}$is the critical solid volume fraction, above which the crystals form a rigid structure. At values of the solid fraction greater than the critical solid fraction, μ_s^* becomes infinitely large, forcing the velocity gradients in the solid phase to vanish. For vanishing solid fractions, Eq. (A5) reduces to that from the Einstein dilute theory, $\mu_s^* = 3.5\mu_l^*$ (Nunziato, 1983). The value of ε_{sp} usually falls between 0.4 and 0.6; a value of 0.5 is used here since lavas rarely erupt with a solid fraction greater than 0.5 (Marsh, 1981).

The numerical method employed is a modification of the SIMPLER algorithm of Spalding (1985). The simulations were done with a Cartesian co-ordinate system and a two-dimensional geometry. Although the growth of small-scales of flow is faster in three dimensions, and hence the flow has more kinetic energy, two-dimensional simulations have been shown to capture the dominant features in prior investigations (Youngs, 1991). Very high resolution was possible by the use of the eight-node Beowulf-configuration parallel computer. Grid refinement studies were performed and satisfactory resolution was obtained for the simulations of aspect ratio with a grid of 500×500, for the aspect ratio of 0.5 it was 500×1000 and for the aspect ratio of 4 it was 500×250. This dense coverage of computational nodes minimizes the effects of numerical diffusion and allows for most scales of the flow to be realized. The implementation of the model equations given above have been verified by comparison with laboratory experiments; see discussion in Bergantz and Ni (1999).

Some of the simulations here reflect inertially dominated conditions, and so a brief discussion of multiphase turbulence is warranted. Crowe et al. (1996) provide a review of the numerical simulation of turbulent multiphase flow. They note that particles can both

suppress and enhance the turbulence intensity depending on the particle loading and the ratio of the particle size to the length scale of the most energetic eddies. Agreement between numerical models and experiments are variable and difficult to generalize (Lahey and Bertodano, 1991). And although some progress has been made on developing general empirical formula for turbulence modulation, currently the NKFS (Nobody Knows For Sure) approach is commonly used. For our simulations, the Stokes numbers are very small, e.g. the relative velocity between phases is small until final stratification is achieved and the eddies were much larger than the particle. Thus the particles follow the flow, and during the most active part of the simulation their influence is like that of a modified mixture viscosity (Tang et al., 1992).

References

Arbaret, L., Diot, H., Bouchez, J.L., Lespinasse, P., Saint Blanquat (de), M., 1997. Analogue 3D simple-shear experiments of magmatic biotite subsurfaces. In: Bouchez, J.L., Hutton, D.H.W., Stephens, W.E. (Eds.), Granite: From Segregation of Melt to Emplacement Fabrics. Kluwer, Dordrecht, pp. 129–144.

Aref, H., Tryggvason, G., 1984. Vortex dynamics of passive and active interfaces. Physica 12D, 59–70.

Argwahl, P.K., O'Neill, B.K., 1988. Transport phenomena in multiparticle system—1. Pressure drop and friction factors: Unifying the hydraulic-radius and submerged object approaches. Chemical Engineering Science 43 (9), 2487–2499.

Barboza, S.A., Bergantz, G.W., 1998. Rheological transitions and the progress of melting of crustal rocks. Earth and Planetary Science Letters 158, 19–29.

Bergantz, G.W., 1990. Melt fraction diagrams: the link between chemical and transport models. In: Nicholls, J., Russell, J.K. (Eds.), Modern Methods of Igneous Petrology: Understanding Magmatic Processes, Reviews in Mineralogy, 24. Mineralogical Society of America, pp. 240–257.

Bergantz, G.W., 1991. Physical and chemical characterization of plutons. In: Kerrick, D.M. (Ed.), Contact Metamorphism, Reviews in Mineralogy, 26. Mineralogical Society of America, pp. 13–42.

Bergantz, G.W., Ni, J., 1999. A numerical study of sedimentation by dripping instabilities in viscous fluids. International Journal of Multiphase Flow 25, 307–320.

Bigg, D., Middleman, S., 1974. Laminar mixing of a pair of fluids in a rectangular cavity. Industrial Engineering Chemical Fundamentals 13, 184–190.

Blumenfeld, P., Bouchez, J.L., 1988. Shear criteria in granite and migmatite deformed in the magmatic and solid stages. Journal of Structural Geology 10, 361–371.

Bremond d'Ars, J., Davy, P., 1991. Gravity instabilities in magma chambers: rheological modeling. Earth and Planetary Science Letters 105, 319–329.

Brown, G.L., Roshko, A., 1974. On density effects and large structure in turbulent mixing layers. Journal of Fluid Mechanics 64, 775–816.

Brown, M., Solar, G.S., 1998. Granite ascent and emplacement during contractional deformation in convergent margins. Journal of Structural Geology 20, 1365–1393.

Campbell, I.H., Turner, J.S., 1986. The influence of viscosity on fountains in magma chambers. Journal of Petrology 27, 1–30.

Celmins, A., 1988. Representation of two-phase flows by volume averaging. International Journal of Multiphase Flow 14, 81–90.

Chien, W.-L., Rising, H., Ottino, J.M., 1986. Laminar mixing and chaotic mixing in several cavity flows. Journal of Fluid Mechanics 170, 355–377.

Crowe, C.T., 1991. The state-of-the-art in the development of numerical models for dispersed phase flows. Proceedings of the First International Conference on Multiphase Flows 3, 49.

Crowe, C.T., Troutt, T.R., Chung, J.N., 1996. Numerical models for two-phase turbulent flows. Annual Reviews of Fluid Mechanics 28, 11–43.

Danckwerts, P.V., 1952. The definition and measurement of some characteristics of mixtures. Applied Science Research A3, 279–296.

Ding, J., Gidaspow, D., 1990. A bubbling fluidization model using kinetic theory of granular flow. American Institute of Chemical Engineers Journal 36, 523–538.

D'Lemos, R.S., Brown, M., Strachan, R.A., 1992. Granite magma generation, ascent and emplacement within a transpressional orogen. Journal of the Geological Society of London 149, 487–490.

Drew, D.A., 1983. Mathematical modeling of two-phase flow. Annual Reviews of Fluid Mechanics 15, 261–291.

Duval, W.M.B., 1992. Numerical study of mixing of two fluids under low gravity. NASA Technical Memorandum 150685, 1–44.

Eichelberger, J.C., Wiebe, R.A., 1999. Chemically zoned ignimbrites: Products of in situ fractionation or silicic replenishment? EOS Transactions of the American Geophysical Union 80 (17 (supplement)), S351.

Elwell, R.W.D., Skelhorn, R.R., Drysdall, A.R., 1960. Inclined granitic pipes in the diorites of Guernsey. Geological Magazine 97, 89–105.

Feder, J., 1988. Fractals. Plenum, New York.

Fernandez, A., 1987. Preferred orientation developed by rigid markers in two-dimensional simple shear strain: a theoretical and experimental study. Tectonophysics 136, 151–158.

Fernandez, A., Fernandez-Catuxo, J., 1997. 3D biotite shape fabric experiments under simple shear strain. In: Bouchez, J.L., Hutton, D.H.W., Stephens, W.E. (Eds.), Granite: From Segregation of Melt to Emplacement Fabrics. Kluwer, Dordrecht, pp. 145–158.

Freeman, B., 1985. The motion of rigid ellipsoidal particles in slow flow. Tectonophysics 113, 163–183.

Frost, T.P., Mahood, G.A., 1987. Field, chemical, and physical constraints on mafic–felsic interaction in the Lamarck Granodiorite, Sierra Nevada, California. Geological Society of America Bulletin 99, 272–291.

Hallot, E., Davy, P., d'Ars, B., Auvray, B., Martin, H., Van Damme, H., 1996. Non-Newtonian effects during injection in partially crystallized magmas. Journal of Volcanology and Geothermal Research 71, 31–44.

Harry, W.T., Richey, J.E., 1963. Magmatic pulses in the emplacement of plutons. Liverpool and Manchester Geological Journal 3, 254–268.

Hassanizadeh, M., Gray, W.G., 1979. General conservation equations for multi-phase systems: 1. Averaging procedure. Advances in Water Research 2, 131–144.

Hill, M., O'Neil, J.R., Noyes, H., Frey, F., Wones, D.R., 1988. Sr, Nd and O isotope variations in compositionally zoned and unzoned plutons in the central Sierra Nevada batholith. American Journal of Science 288-A, 213–241.

Hill, R.I., 1988. San Jacinto Intrusive Complex 1. Geology and mineral chemistry, and a model for intermittent recharge of tonalitic magma chambers. Journal of Geophysical Research 93 (B9), 10325–10348.

Hill, R.I., Silver, L.T., 1988. San Jacinto Intrusive Complex 3. Constraints on crustal magma chamber processes from strontium isotope heterogeneity. Journal of Geophysical Research 93 (B9), 10373–10388.

Hills, R.N., Roberts, P.H., 1988. On the use of Fick's law in regions of mixed phase. International Communications in Heat and Mass Transfer 15, 113–119.

Hogan, J.P., Price, J.D., Gilbert, M.C., 1998. Magma traps and driving pressure: consequences for pluton shape and emplacement in an extensional regime. Journal of Structural Geology 20, 1155–1168.

Huppert, H.E., Sparks, R.S.J., Whitehead, J.A., Hallworth, M.A., 1986. Replenishment of magma chambers by light inputs. Journal of Geophysical Research 91, 6113–6122.

Ildefonse, B., Arbaret, L., Diot, H., 1997. Rigid particles in simple shear flow: Is their preferred orientation periodic or steady-state? In: Bouchez, J.L., Hutton, D.H.W., Stephens, W.E. (Eds.), Granite: From Segregation of Melt to Emplacement Fabrics. Kluwer, Dordrecht, pp. 177–188.

Ildefonse, B., Fernandez, A., 1988. Influence of the concentration of rigid markers in a viscous medium on the production of preferred orientations. An experimental contribution, 1. Non-coaxial strain. Bulletin Geological Institute of the University of Uppsala 14, 55–60.

Ildefonse, B., Launeau, P., Bouchez, J.-L., 1992. Effect of mechanical interactions on the development of shape preferred orientations: a two dimensional experimental approach. Journal of Structural Geology 14, 73–83.

Ishii, M., 1975. Thermo-fluid Dynamic Theory of Two-Phase Flow. Eyrolles, Paris.

Jezek, J., Schulmann, K., Segeth, K., 1996. Fabric evolution of rigid particles during mixed coaxial and simple shear flows. Tectonophysics 257, 203–220.

John, B.E., Stunitz, H., 1997. Magmatic fracturing and small-scale melt segregation during pluton emplacement: evidence from the Adamello massif (Italy). In: Bouchez, J.L., Hutton, D.H.W., Stephens, W.E. (Eds.), Granite: From Segregation of Melt to Emplacement Fabrics. Kluwer, Dordrecht, pp. 55–74.

Khakar, D.V., Rising, H., Ottino, J.M., 1986. Analysis of chaotic mixing in two model systems. Journal of Fluid Mechanics 172, 419–451.

Knesel, K.M., Davidson, J.P., Duffield, W.A., 1999. Evolution of silicic magma through assimilation and subsequent recharge: Evidence from Sr isotopes in sanadine phenocrysts, Taylor Creek rhyolite, NM. Journal of Petrology 40, 773–786.

Lahey, R.T., Bertodano, M.L., 1991. The prediction of phase distribution using the two-fluid model., ASME/JSME Thermal Engineering proceedings, 193-200.

Linden, P.F., Redondo, J.M., Youngs, D.L., 1994. Molecular mixing in Rayleigh–Taylor instability. Journal of Fluid Mechanics 265, 97–124.

Macias, S., 1996. The Sonora Intrusive Suite: Constraints on the Assembly of a Late Cretaceous, Concentrically Zoned Granitic Pluton in the Sierra Nevada Batholith. Unpublished M.S. thesis, University of Washington.

Mahmood, A., 1985. Emplacement of the zoned Zaer pluton, Morocco. Geological Society of America Bulletin 96, 931–939.

Mahood, G.A., 1990. Second reply to comment of R.S.J. Sparks, H.E. Huppert and C.J.N. Wilson on "Evidence for long residence times of rhyolitic magma in the Long Valley magmatic system: the isotopic record in the precaldera lavas of Glass Mountain". Earth and Planetary Science Letters 99, 395–399.

Marsh, B.D., 1981. On the crystallinity, probability of occurrence, and rheology of lava and magma. Contributions in Mineralogy and Petrology 78, 85–98.

McEwan, A.D., 1983a. Internal mixing in stratified fluids. Journal of Fluid Mechanics 128, 59–80.

McEwan, A.D., 1983b. The kinematics of stratified mixing through internal wave-breaking. Journal of Fluid Mechanics 128, 47–57.

Moses, E., Zocchi, G., Libchaber, A., 1993. An experimental study of laminar plumes. Journal of Fluid Mechanics 251, 581–601.

Ni, J., Beckermann, C., 1991. A volume-averaged two-phase model for transport phenomena during solidification. Metallurgical Transactions B 22B, 349–361.

Nicolas, A., 1992. Kinematics in magmatic rocks with special reference to gabbros. Journal of Petrology 33, 891–915.

Nunziato, J.W., 1983. A multiphase mixture theory for fluid–particle flows. In: Meyer, R.E. (Ed.), Theory of Dispersed Multiphase Flow. Academic Press, New York, pp. 191–226.

Oldenburg, C.M., Spera, F.J., Yuen, D.A., Sewell, G., 1989. Dynamic mixing in magma bodies: Theory, simulations and implications. Journal of Geophysical Research 94, 9215–9236.

Ottino, J.M., 1989. The Kinematics of Mixing: Stretching, Chaos, and Transport. Cambridge University Press, Cambridge.

Ottino, J.M., Leong, C.W., Rising, H., Swanson, P.D., 1988. Morphological structures produced by mixing in chaotic flows. Nature 333, 419–425.

Ottino, J.M., Ranz, W.E., Macosko, W., 1979. A lamellar model for analysis of liquid–liquid mixing. Chemical Engineering Science 34, 877–890.

Paterson, S.R., Fowler, T.K., Schmidt, K.L., Yoshinobu, A.S., Yuan, E.S., Miller, R.B., 1998. Interpreting magmatic fabric patterns in plutons. Lithos 44, 53–82.

Paterson, S.R., Miller, R.B., 1998. Midcrustal magmatic sheets in the Cascades Mountains, Washington: implications for magma ascent. Journal of Structural Geology 20, 1345–1363.

Pembroke, J.W., D'Lemos, R.S., 1995. Recognition and significance of mixing in granites. In: Brown, M., Piccoli, P. (Eds.), The Origin of Granites and Related Rocks, Third Hutton Symposium Abstracts, 1129. US Geological Survey Circular, Washington, p. 113.

Petford, N., Clemens, J.D., Vigneresse, J.L., 1997. Application of information theory to the formation of granitic rocks. In: Bouchez, J.L., Hutton, D.W.H., Stephens, W.E. (Eds.), Granite: From Segregation of Melt to Emplacement Fabrics. Kluwer, Dordrecht, pp. 3–10.

Ramsay, J.G., 1989. Emplacement kinematics of a granite diapir: the Chindamora batholith, Zimbabwe. Journal of Structural Geology 11, 191–209.

Saint Blanquat (de), M., Tikoff, B., 1997. Development of magmatic to solid-state fabrics during syntectonic emplacement of the Mono Creek granite, Sierra Nevada batholith. In: Bouchez, J.L., Hutton, D.H.W., Stephens, W.E. (Eds.), Granite: From Segregation of Melt to Emplacement Fabrics. Kluwer, Dordrecht, pp. 231–252.

Sawyer, E.W., 1998. Formation and evolution of granite magmas during crustal reworking: the significance of diatexites. Journal of Petrology 39, 1147–1168.

Schwindinger, K.R., 1999. Particle dynamics and aggregation of crystals in a magma chamber with application to Kilauea Iki olivines. Journal of Volcanology and Geothermal Research 88, 209–238.

Shimizu, M., Gastil, G., 1990. Recent advances in concepts concerning zoned plutons in Japan and Southern and Baja California. The University Museum, The University of Tokyo, Nature and Culture, no. 2, 244.

Snider, D.M., Andrews, M.J., 1994. Rayleigh–Taylor and shear driven mixing with an unstable thermal stratification. Physics of Fluids 6, 3324–3334.

Sonnenthal, E.L., McBirney, A.R., 1998. The Skaergaard Layered Series. Part IV. Reaction–transport simulations of foundered blocks. Journal of Petrology 39, 633–661.

Spalding, D.B., 1985. Computer simulation of two-phase flows with special reference to nuclear reactor systems. In: Lewis, R.W., Morgan, K., Johnsen, J.A., Smith, W.R. (Eds.), Computational Techniques in Heat Transfer. Pineridge Press, Swansea, pp. 1–44.

Sparks, R.S.J., Marshall, L., 1986. Thermal and mechanical con-

straints on mixing between mafic and silicic magmas. Journal of Volcanology and Geothermal Research 29, 99–124.

Tang, L., Wen, F., Yang, Y., Crowe, C.T., Chung, J.N., Troutt, T.R., 1992. Self-organizing particle dispersion mechanism in free shear flows. Physics of Fluids A4, 2244–2249.

Vaughan, A.M.P., Thistlewood, L., Millar, I.L., 1995. Small-scale convection at the interface between stratified layers of mafic and silicic magma, Campbell Ridges, NW Palmer Land, Antarctic Peninsula: syn-magmatic way-up criteria. Journal of Structural Geology 17, 1071–1075.

Vigneresse, J.L., Barbey, P., Cuney, M., 1996. Rheological transitions during partial melting and crystallization with application to the felsic magma segregation and transfer. Journal of Petrology 37, 1579–1600.

Wiebe, R.A., Collins, W.J., 1998. Depositional features and stratigraphic sections in granitic plutons: implications for the emplacement and crystallization of granitic magma. Journal of Structural Geology 20, 1273–1289.

Wiebe, R.A., Ulrich, R., 1997. Origin of composite dikes in the Gouldsboro granite, coastal Maine. Lithos 40, 157–178.

Yoshinobu, A.S., Okaya, D.A., Paterson, S.R., 1998. Modeling the thermal evolution of fault-controlled magma emplacement models: implications for the solidification of granitoid plutons. Journal of Structural Geology 20, 1205–1218.

Youngs, D.L., 1991. Three-dimensional numerical simulation of turbulent mixing by Rayleigh–Taylor instability. Physics of Fluids A3 (5), 1312–1320.